Proc. Natl. Acad. Sci. USA
Vol. 94, pp. 5662–5666, May 1997
Cell Biology

Characterization of *VPS41*, a gene required for vacuolar trafficking and high-affinity iron transport in yeast

DEREK C. RADISKY*, WILLIAM B. SNYDER†, SCOTT D. EMR†, AND JERRY KAPLAN*‡

*Department of Pathology, University of Utah Health Sciences Center, Salt Lake City, UT 84132; and †Howard Hughes Medical Institute, Division of Cellular and Molecular Medicine, University of California at San Diego School of Medicine, La Jolla, CA 92023-0668

Communicated by Stuart A. Kornfeld, Washington University School of Medicine, St. Louis, MO, March 17, 1997 (received for review February 4, 1997)

ABSTRACT **Mutations in the yeast gene *VPS41* give rise to poor growth on low iron medium, severe alterations in vacuolar morphology, and cause the missorting of membranous and soluble vacuolar proteins. Our studies predict that *VPS41* encodes a hydrophilic protein of 992 amino acids that contains no obvious signal sequence or hydrophobic domains. The deduced Vps41p sequence contains a domain rich in glutamic and aspartic residues, as well as a domain with resemblance to a region of clathrin heavy chain. We have also identified and sequenced putative *VPS41* homologues from *Caenorhabditis elegans*, plants, and humans. The *VPS41* homologues (but not the yeast *VPS41* itself) contain a conserved cysteine-rich RING-H2 zinc finger at their COOH termini. Biochemical experiments suggest that *VPS41* functions in post-Golgi protein processing: the deletion mutant exhibits defective high affinity transport due to impaired Fet3p activity and also exhibits defects in the processing and sorting of multiple vacuolar hydrolases.**

High-affinity iron uptake in *Saccharomyces cerevisiae* is mediated by the transmembrane transporter Ftr1p and the cell surface ferroxidase Fet3p (1). The multicopper oxidase Fet3p catalyzes the oxidation of ferrous iron to ferric iron, which is then transported across the membrane by Ftr1p. The catalytic activity of Fet3p requires the products of *CTR1* (2), the cell surface copper transporter, and *CCC2* (3), which transports copper into intracellular vesicles during the assembly of Fet3p. The *CCC2* gene product is homologous to the mammalian Wilson disease and Menkes disease gene products (3). Mutations in either of the human genes result in defective copper transport and incomplete copper insertion into ceruloplasmin (4), a mammalian protein with homology to Fet3p (3).

To dissect the steps involved in the intracellular processing of Fet3p and other proteins involved in high-affinity iron transport, we have used a genetic screen that selects for mutants that are unable to grow on low-iron medium but can grow on high-iron medium (*fet* mutants, for ferrous transport). Growth on low-iron medium requires the proper assembly and localization of the Fet3p/Ftr1p transport system, but growth on iron-rich medium can occur by the low-affinity Fet4p iron transporter. From our *fet* screen, we isolated many mutants that had normal *FET3* and *FTR1* genes, but exhibited greatly reduced high-affinity iron transport. One such mutant was used to identify a gene required for the proper assembly and targeting of the high-affinity transport system. This gene, *VPS41*, which is essential for the functioning of Fet3p, is conserved across all species tested and is expressed in all human tissues. Yeast strains with a disrupted *VPS41* show abnormalities in both vacuolar morphology and post-Golgi trafficking of vacuolar components. Our results suggest that the elements of the yeast high-affinity iron transport system require the post-Golgi-vacuolar pathway for proper functioning, and that the *fet* screen offers a facile way to identify new genes involved in the post-Golgi-vacuolar pathway.

MATERIALS AND METHODS

Strains and Media. The *S. cerevisiae* strains used in this study were derived from SEY6210, DY150, and DY1457, as previously described (5, 6). Luria–Bertani medium was used to propagate *Escherichia coli* strains DH5α and HB101 and the strains were supplemented with antibiotics as required [Miller (7)]. Yeast extract-peptone-dextrose (YPD), or yeast nitrogen base was used for the standard growth of *S. cerevisiae* and supplemented as needed (8). Low-iron growth medium was made by the addition of bathophenanthroline sulfonate (BPS) to YPD (9). The *fet2* mutant was isolated in a screen that selected for resistance to streptonigrin as described previously (5). To generate *vps41*Δ*1*, a *Nhe*I–*Pvu*II fragment containing *VPS41* in pBluescript KS(+) was digested with *Pst*I and *Hin*dIII, and a *Hin*dIII/*Pst*I fragment containing *LEU2* was ligated into the gap. This construct was then digested with *Sca*I and *Bgl*II and transformed into SEY6210. To generate *vps41*Δ*2*, a *Nhe*I–*Nhe*I fragment containing *VPS41* was digested with *Eco*NI and *Sse*8387I, filled in with Klenow, and a blunt-ended fragment containing *URA3* was ligated into the gap and then transformed into DY150.

Reagents and Materials. DNA restriction and modifying enzymes were obtained from New England Biolabs, Boehringer Mannheim, or Promega. CDCFDA and FM4–64 were obtained from Molecular Probes. Trans ^{35}S-label was obtained from ICN, and [α-^{32}P]dCTP was from Amersham. The antiserum to carboxypeptidase Y has been described previously (10). All other reagents were from Sigma.

Cloning of VPS41 and Homologues. DNA transformations of *E. coli* and *S. cerevisiae* were performed by standard procedures (11). The *VPS41* gene was cloned by transformation of *fet2* with a yeast genomic library and selection for complementation of the low-iron growth phenotype using techniques described previously (5). A single unique plasmid was isolated and then shown to be derived from chromosome 4 by sequencing the ends of the plasmid insert. Subcloning mapped a minimum *fet2* complementing activity to a *Nhe*I–*Nhe*I fragment containing only the single, large ORF YDR080W. *VPS41* was also cloned by complementation of the secretion of CPY-Inv from a *suc2* version of one of the original

The publication costs of this article were defrayed in part by page charge payment. This article must therefore be hereby marked "*advertisement*" in accordance with 18 U.S.C. §1734 solely to indicate this fact.

0027-8424/97/945662-5$2.00/0
PNAS is available online at **http://www.pnas.org**.

Abbreviations: CPY, carboxypeptidase Y; PrA, proteinase A; ALP, alkaline phosphatase; YPD, yeast extract-peptone-dextrose; PPD, paraphenylene diamine.

Data deposition: The sequences reported in this paper have been deposited in the GenBank database [accession nos. U83709 (*hVPS41*), U86662 (*tVPS41*), and U86663 (*Arabidopsis* EST)].

‡To whom reprint requests should be addressed.

vps41 mutant strains (*vpl20–1*) (12). A complementing fragment again was determined to be derived from chromosome 4, and a minimum complementing *Nhe*I–*Pvu*II fragment again contained only YDR080W.

The human homologue of *VPS41* (*hVPS41*) was identified by similarity of the predicted sequence of Vps41p with expressed sequence tag (EST) 127498 from the dbEST database, which was derived from normalized human fetal liver and spleen library (T. Newman, Washington University). This clone was obtained from the Lawrence Livermore National Lab and was found to contain a 1.6-kb insert. This cDNA was used to probe a λZAPII library that was oligo(dT)- and random-primed from human heart mRNA (Stratagene). Exhaustive probing of this library combined with a rapid amplification of cDNA ends (RACE) strategy was used to isolate the *hVPS41* sequence.

Similarly, the tomato (*Lycopersicon esculentum*) homologue of *VPS41* (*tVPS41*) was identified by similarity of the predicted sequence of Vps41p with EST 89D22T7 from the dbEST database, which was derived from an *Arabidopsis thaliana* library (T. Newman). The clone was obtained from the Arabidopsis Biological Resource Center at Ohio State and was found to contain a 1.2-kb insert, and was used to probe a λZAPII library that was oligo(dT)-primed from tomato mRNA. The library contained multiple, full-length copies of the *tVPS41* sequence.

Iron Transport and Growth Assays. Cultures were grown to midlog phase in YPD, either harvested or transferred to YPDBPS(0) for a 4-hr induction, and then harvested. Iron uptake was assessed essentially as previously described (5), in the presence of 1 μM ascorbate and in the absence of copper. For growth on synthetic LIM medium and LIM medium supplemented with $FeCl_3$ and $CuSO_4$, cells were washed with water and placed at a dilution of 1,000 cells per drop. The preparation of LIM is described in a previous report (9).

Cell Labeling and Immunoprecipitations. Yeast cells were grown to an A_{600} of 0.6–0.7 in yeast nitrogen base containing the required amino acids. Cells were harvested, labeled with Trans ^{35}S-label for 10 min at 30°C, chased for 0 min and 45 min, and converted to spheroplasts as described previously (13). Carboxypeptidase Y (CPY), proteinase A (PrA), and alkaline phosphatase (ALP) were immunoprecipitated by established methods (14, 15).

Vacuolar Staining with FM4–64 and Electron Microscopy. Procedures for staining of vacuoles with FM4–64 have been described previously (16). For electron microscopy cells were grown at 26°C in log phase. Cells were harvested and prepared as described previously (13).

RESULTS

Characterization of *VPS41*. We selected the mutant *fet2*, which showed a growth defect on low-iron medium, and identified *VPS41* by complementation of the low-iron growth phenotype. The deletion strain *vps41Δ2* showed a more severe growth defect than *fet2*, with deficient growth on both high- and low-iron medium. That *VPS41* was the normal allele of *fet2* was confirmed by demonstrating that *vps41Δ2* cells complimented with the rescued *fet2* allele showed normal growth on iron-replete medium, but defective growth on low-iron medium. The different phenotypes observed in the *fet2* and *vps41Δ2* alleles suggests that the original *fet2* mutant may retain some function, although the mutant allele has not been genetically characterized. The phenotype of poor growth on low iron can be caused either by a deficiency in iron transport activity or by a metabolic defect that confers sensitivity to low-iron conditions. A role in high-affinity iron transport for *VPS41* was demonstrated by comparison of iron uptake between wild-type and *vps41Δ2* deletion strains (Fig. 1). In high-iron conditions (YPD), iron transport is mediated primarily by Fet4p and is unaffected by the deletion of *VPS41*.

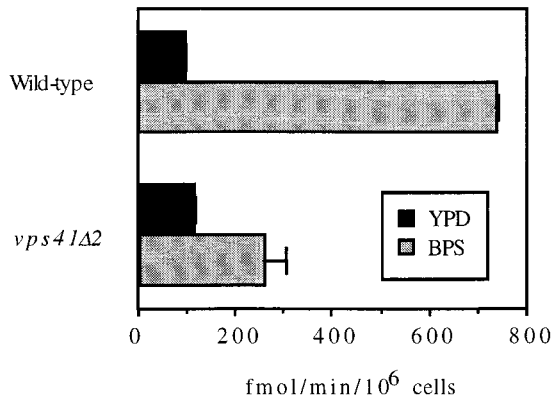

FIG. 1. Iron transport in wild-type yeast and the *vps41Δ2* strain. Cells were grown to midlog phase in iron replete (YPD) media, and then assayed immediately or incubated for 4 hr in iron-limited (BPS) media. The cells were harvested and iron transport was assayed using 0.5 μM iron in the absence of ascorbate and copper.

However, incubation in iron-deficient media (BPS) produced a marked induction of transporter activity in wild-type cells, whereas the deletion strain exhibited a defect in iron transport.

Identification of *VPS41* Homologues. A TBLASTN computer search of the swissprot database revealed several high-probability matches to the predicted amino acid sequence of *VPS41*. One ORF, designated as F32A6.3, published as part of the *C. elegans* sequencing project (17), codes for a protein of unknown function. This sequence is homologous throughout its length to *VPS41*; we will subsequently refer to this gene as *cVPS41*.

A search of dbEST also identified partial human EST clones, including S53, a cDNA in the region of the early-onset Alzheimer disease gene (18). As the database sequence of *hVPS41* was incomplete, multiple rounds of cloning from a human heart λZAPII library and RACE were necessary to obtain a full-length 3.5-kb sequence coding for *hVPS41*. This insert was used to probe a multiple-tissue Northern blot (CLONTECH) and detected 3.5-kb transcripts equally expressed in all tissues tested. Additionally, since the EST S53 has been mapped, we know that *hVPS41* is on human chromosome 14q23 (18).

The National Center for Biotechnology Information search also identified an *A. thaliana* EST (19). Only a few hundred nucleotides were available from the database for this sequence, so we obtained the clone, sequenced it, and used the insert to probe a tomato λZAPII library. From this library, we obtained a clone with a 3.3-kb insert containing *tVPS41*.

Comparison of *VPS41* Homologues. Sequence alignment of the predicted sequences of Vps41p, cVps41p, tVps41p, and hVps41p revealed significant structural similarity across the length of the protein (Fig. 2), although *hVPS41* did not complement the phenotype of *vps41Δ2*. Most interesting is the region between amino acids 806 and 882 of the Vps41p predicted sequence: across all four species, the sequence similarity exceeds 70%, and identity exceeds 30%. This highly conserved sequence in Vps41p and homologues is also similar to residues 1036–1118 in human clathrin heavy chain (50% similarity between Vps41p homologues and clathrin). A sequence motif found in the Vps41p homologues but not in Vps41p itself is the RING-H2 motif, a zinc finger-like motif previously identified in *VPS8*, *VPS18,* and *VPS11* (20). Other proteins containing this motif have been found to associate with endosomes, the vacuole, or other vesicular structures (21).

Another striking region was a 19-residue sequence containing only glutamic and aspartic acids (positions 78–97 in Vps41p). More than 600 known protein sequences contain such glu, asp-rich domains, and although these domains have no known function, many proteins containing such acidic regions bind calcium or other metals. This motif is found in

FIG. 2. Alignment of Vps41p, cVps41p, tVps41p, and hVps41p.

Vps41p, tVps41p, and hVps41p, but not cVps41p. Interestingly, a second glu, asp-rich sequence is also found between the second and third metal binding motifs in the RING-H2 finger of tVps41p; a similar motif exists in the homologous region of our partial *A. thaliana* Vps41p sequence (data not shown).

Characterization of the *vps* Phenotype. Originally, *vps41* alleles were obtained from screens of mutants that secrete resident vacuolar proteins. We examined the sorting of three vacuolar hydrolases, ALP, CPY, and PrA in yeast strains that were wild-type, *vps41Δ1*, and *vps41Δ1* complemented with centromeric *VPS41* (Fig. 3). Wild-type cells and *vps41Δ1* complemented by *VPS41* showed nearly identical sorting and processing of all hydrolases examined. In contrast, *vps41Δ1* strains showed no maturation of CPY or ALP even after a 40-min chase. In addition, approximately 60% of the newly synthesized CPY was secreted as the Golgi modified p2 form, indicating a partial defect for vacuolar protein sorting in the Golgi. ALP is a type II integral membrane protein and is not released from whole cells; its presence in the intracellular fractions is therefore expected even when vacuolar localization is not achieved. PrA, the other hydrolase examined, shows significant intracellular accumulation of precursor PrA and some mature protein. A significant portion of PrA is released to the extracellular media following the 40-min chase indicating a defect in *vps41Δ1* strains for the sorting of PrA from the Golgi to the vacuole.

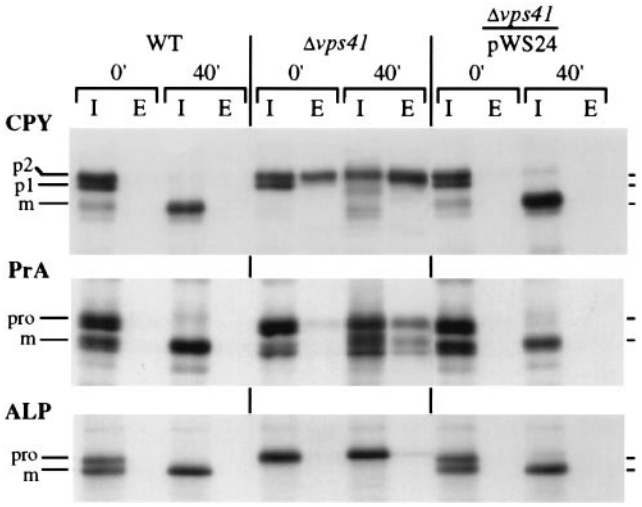

FIG. 3. Pulse–chase analysis of vacuolar hydrolases. Wild-type cells, *vps41Δ1* deletion mutants, and *vps41Δ1* cells complemented with *VPS41* (pWS24) were grown to midlog phase at 30°C, pulse-labeled with Trans ^{35}S-label for 10 min, and chased with excess unlabeled cysteine and methionine, and cells were harvested 0 min and 40 min after the addition of the chase medium. The samples were then separated into intracellular (I) and extracellular (E) fractions, and specific proteins were immunoprecipitated and applied to SDS/PAGE and autoradiography.

A common consequence of certain mutations that impair trafficking of vacuolar proteins is abnormal vacuolar morphology (12). Examination of *vps41Δ1* mutants stained with the fluorescent dye FM4–64, a useful membrane stain for the vacuole (16), revealed extensive fragmentation of the vacuole (Fig. 4 *A* and *B*). The observation of 20–50 small, brightly staining compartments in *vps41Δ1* mutants is consistent with its previous classification as a class B *vps* mutant (12). Vacuolar fragmentation is not seen in *vps41Δ1* mutants complemented with a centromeric plasmid containing *VPS41* (Fig. 4 *C* and *D*). Examination of *vps41Δ1* mutants by electron microscopy revealed the presence of many small membrane-bound compartments (Fig. 4*E*). Wild-type or complemented deletion mutants have 1–3 electron dense vacuolar compartments (Fig. 4*F*; for wild types, see refs. 13 and 22–24). The membrane-bound compartments in *vps41Δ1* cells likely correspond to the brightly staining compartments observed in Fig. 4*A*, the fragmented vacuoles, and related structures that accumulate in the absence of Vps41p.

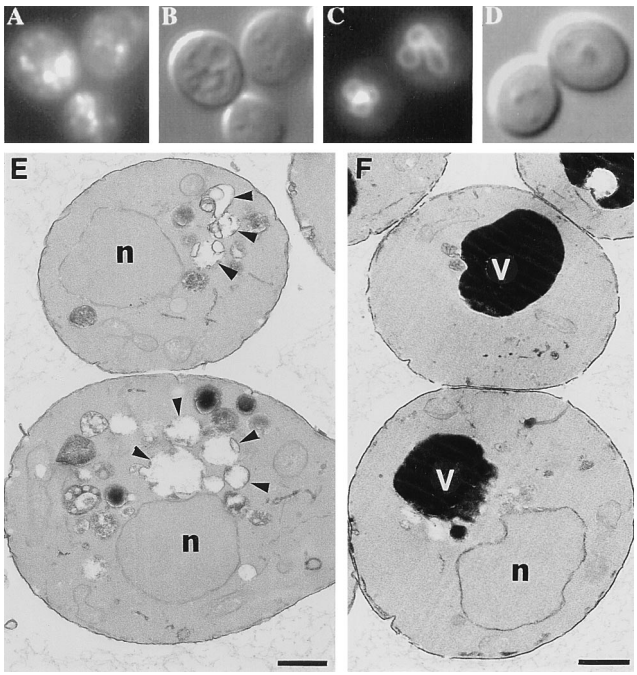

FIG. 4. Vacuolar morphology examined by staining with the vacuole-specific dye FM4–64 (*A* and *C*), by Nomarski imaging (*B* and *D*), or by electron microscopy (*E* and *F*) of *vps41Δ1* deletion mutants (*A*, *B*, and *E*) or *vps41Δ1* complemented with *VPS41* (*C*, *D*, and *F*).

Cause of Low-Iron Growth Defect. Because *vps41Δ1* interferes with the processing of vacuolar hydrolases, and because Fet3p requires several distinct posttranslational processing events, including glycosylation and copper loading, it seemed possible that the defect in high-affinity iron transport in *vps41* deletion cells was due in part to improperly processed, and thus inactive, Fet3p. Northern blot analysis showed that the concentration of *VPS41* mRNA was independent of iron content in the media, and that wild-type, *fet2*, and *vps41Δ2* cells had normal low-iron induction of *FET3* mRNA (data not shown). Western blot analysis of both wild-type and *vps41Δ2* cells induced for expression of the high-affinity transport system revealed a strongly staining glycosylated Fet3p band as well as a weakly staining unglycosylated Fet3p band (data not shown; ref. 2). Oxidase activity of Fet3p was tested by assaying the oxidation of paraphenylene diamine (PPD), an organic substrate used as an oxidase indicator (3). Oxidation of PPD by membranes isolated from *vps41Δ2* cells was found to be reduced to the level of *fet3Δ* cells (Fig. 5*a*). That Fet3p from *vps41Δ2* cells was normally glycosylated but lacked PPD activity suggested that the deletion mutant might be blocked in the processing step in which copper is incorporated into apoFet3p. Consistent with this hypothesis, we found that the low-iron growth defect of *vps41Δ2* could be overcome by growth in the presence of high copper (Fig. 5*b*). High concentrations of copper also rescued the low-iron growth defect of *ccc2Δ* (3), which is known to be defective in intracellular Fet3p copper incorporation, but did not rescue *fet3Δ*.

DISCUSSION

We have identified *VPS41*, which is required for growth on low-iron medium, correct vacuolar protein sorting, and normal vacuolar morphology. Cells containing deletions of *VPS41* show normal induction of *FET3* mRNA and protein but defective Fet3p function, both in oxidase activity and in iron transport. The reduced PPD oxidase activity in the *vps41Δ2* deletion suggests that its low-iron growth phenotype results from defective functioning of Fet3p. The observation that high copper can rescue the mutant indicates that the defect is due to a lack of copper incorporation into Fet3p.

The activity of Fet3p requires intracellular copper incorporation, which is dependent on the copper transporter Ccc2p. Analogously, copper incorporation into ceruloplasmin, the mammalian Fet3p homologue, occurs in an intracellular compartment and requires the products of the Menkes and Wilson disease genes (4), which are copper transporters homologous to Ccc2p. The observation that high-copper medium can rescue the low-iron growth phenotype of *vps41* deletion mutants suggests that the compromised high-affinity iron uptake in these cells results from a lack of copper incorporation into Fet3p, possibly because *VPS41* is required for proper sorting of Fet3p or Ccc2p. These proteins may require the environment of the prevacuolar endosome for their function. Alteration of delivery to, or function of, this compartment in *vps41* mutants would result in the observed defects in Fet3p function.

In the absence of *VPS41*, Fet3p and CPY are glycosylated, indicating that the processing defect occurs after the trans-Golgi network. Class E *vps* mutants, which show defects in vesicular traffic from the prevacuolar endosome to the vacuole (12), show no deficiency of growth on low-iron medium, and therefore, these mutants must process Fet3p normally. The

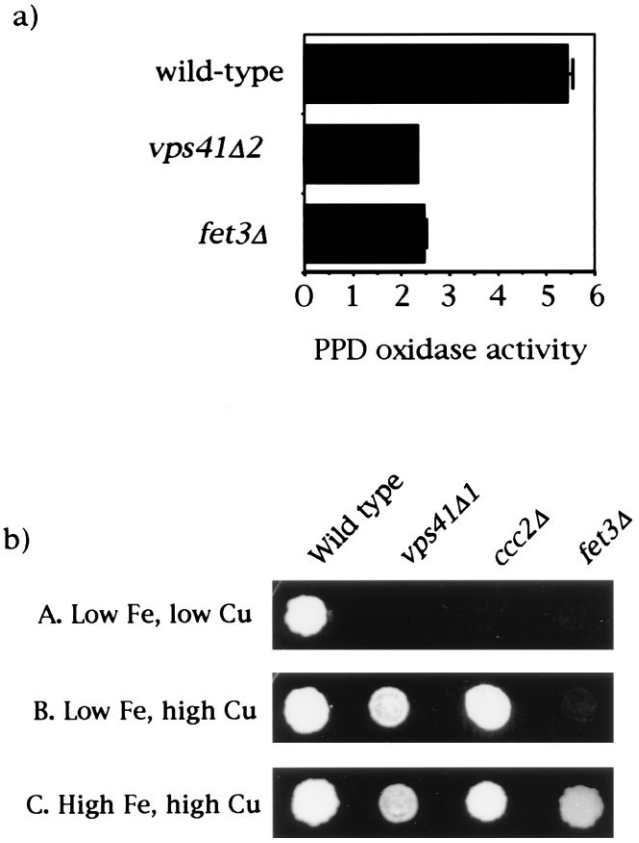

FIG. 5. Effect of *VPS41* deletion on Fet3p activity. (*a*) PPD oxidase activity of wild-type, *vps41*Δ*2*, and *fet3*Δ cells. Five milligrams of a crude membrane fraction obtained from cells grown in low-iron medium was incubated with 0.05% PPD in 100 mM NaOAc (pH 5.7) for 12 hr and quantified by A_{570}. (*b*) Metal-dependent growth phenotypes of *vps41*Δ*1*. The effect of added iron or copper on growth on LIM medium was determined for the indicated yeast strains. A, 5 μM Fe, 0.125 μM Cu; B, 5 μM Fe, 500 μM Cu; C, 50 μM Fe, 500 μM Cu.

prevacuolar endosome is an organelle analogous to the mammalian late endosome, which may be one of the post-Golgi vesicles identified to contain the Menkes gene product (25). On the basis of these observations, we surmise that the Fet3p defect in *VPS41* deletion cells is due to a defect in the function of the prevacuolar endosome. This hypothesis is consistent with the observed defects in vacuolar protein sorting. It is possible that the primary defect in *VPS41* deletion cells is assembly of the iron uptake system and that high-affinity iron uptake (or at least a functional Fet3p) is necessary for vacuolar protein sorting, although this hypothesis is unlikely, as *fet3* mutants do not display *vps* phenotypes.

Homologues of *VPS41* have been found in all species examined, and the mammalian *hVPS41* mRNA was found in all tissues examined. Vps41p and its homologues have similarity with other proteins involved in vesicular traffic. The most conserved region between Vps41p and its homologues is also similar to a region of clathrin heavy chain, which is involved in protein targeting from the trans-Golgi network to the vacuole (26). On the basis of this homology and the biochemical defects in *vps41* mutants, we hypothesize that Vps41p may function in the packaging of some vacuolar proteins into transport intermediates such as vesicles.

It is striking that while all of the homologues contain a RING-H2 finger, this motif is lacking in yeast Vps41p. Since it seems very unlikely that a motif conserved across species as diverse as *C. elegans* and humans should be unnecessary for the function of Vps41p, it seems probable that the RING-H2 motif in yeast is provided by an unidentified protein complexed to Vps41p. Further support for the hypothesis that functional regions may be conserved within a Vps41p–protein complex can be inferred from the lack of a glu, asp-rich domain in cVps41p; we predict that the *C. elegans* equivalent of the Vps41p-associated protein will be found to contain an acidic region. Our *fet* screen may identify the yeast Vps41p-associated protein, since a mutation in such a gene might produce the same phenotype as *fet2*. Examination of *fet* mutants stained with FM4–64 for *fet2*-like vacuolar appearance may identify mutations in the Vps41p-associated protein, and complementation of the low-iron phenotype of *fet* mutants will identify the defective gene. Indeed, other *fet* mutants in our collection have been found to exhibit the *vps* phenotype, showing defects in both protein sorting and vacuolar morphology (data not shown).

We thank J. Michael McCaffery for electron microscopy analysis, Tama Fox for assistance with cloning *tVPS41*, and members of the J.K. and S.D.E. lab for helpful discussion. W.B.S. is supported as a postdoctoral fellow of the American Cancer Society. This work was supported by grants from the National Institutes of Health (HL26922 and DK30534 to J.K., GM32703 and CA58689 to S.D.E.). S.D.E. is supported as an investigator of the Howard Hughes Medical Institute.

1. Stearman, R., Yuan, D. S., Yamaguchi-Iwai, Y., Klausner, R. D. & Dancis, A. (1996) *Science* **271,** 1552–1557.
2. Dancis, A., Yuan, D. S., Haile, D., Askwith, C., Eide, D., Moehle, C., Kaplan, J. & Klausner, R. D. (1994) *Cell* **76,** 393–402.
3. Yuan, D. S., Stearman R., Dancis, A., Dunn, T., Beeler, T. & Klausner, R. D. (1995) *Proc. Natl. Acad. Sci. USA* **92,** 2632–2636.
4. Harris, Z. L. & Gitlin, J. D. (1996) *Am. J. Clin. Nutr.* **63,** 836S–841S.
5. Askwith, C., Eide, D, Ho, A. V., Bernard, P. S., Li, L., Davis-Kaplan, S., Sipe, D. M. & Kaplan, J., (1994) *Cell* **76,** 3018–3023.
6. Robinson, J. S., Klionsky, D. J., Banta, L. M. & Emr, S. D. (1988) *Mol. Cell. Biol.* **8,** 4936–4948.
7. Miller, J. (1972) *Experiments in Molecular Genetics* (Cold Spring Harbor Lab. Press, Cold Spring Harbor, NY).
8. Sherman, F., Fink, G. R. & Lawrence, L. W. (1986) *Laboratory Course Manual for Methods in Yeast Genetics* (Cold Spring Harbor Lab. Press, Cold Spring Harbor, NY).
9. Eide, D. & Guarante, L. (1992) *J. Gen. Microbiol.* **138,** 34–54.
10. Klionsky, D. J. & Emr, S. D., (1989) *EMBO J.* **8,** 2241–2250.
11. Sambrook, J., Fritsch, E. F. & Maniatis, T. (1989) *Molecular Cloning: A Laboratory Manual* (Cold Spring Harbor Lab. Press, Cold Spring Harbor, NY), 2nd Ed.
12. Raymond, C. K., Howald-Stevenson, I., Vater, C. A. & Stevens, T. H. (1992) *Mol. Biol. Cell.* **3,** 1389–1402.
13. Cowles, C. R., Emr, S. D. & Horazdovsky, B. F. (1994) *J. Cell Sci.* **107,** 3449–3459.
14. Klionsky, D. J., Banta, L. M. & Emr, S. D. (1988) *Mol. Cell. Biol.* **8,** 2105–2116.
15. Klionsky, D. J. and Emr, S. D. (1989) *EMBO J.* **8,** 2241–2250.
16. Vita, T. A. & Emr, S. D. (1995) *J. Cell Biol.* **128,** 779–792.
17. Wilson, R., Ainscough, R., Anderson, K., Baynes, C., Berks, M., *et al.* (1994) *Nature (London)* **368,** 32–38.
18. Sherington, R., Rogaev, E. I., Liang, Y., Rogaeva, E. A., Levesque, G. *et al.* (1995) *Nature (London)* **375,** 754–760.
19. Newman, T., de Bruijn, F. J., Green, P., Keegstra, K., Kende, H., McIntosh, L., Ohlrogge, J., Raikhel, N., Somerville, S., Tomashow, M., Retzel, E. & Somerville, C. (1994) *Plant Physiol.* **106,** 1241–1255.
20. Horazdovsky, B. F., Cowles, C. R., Mustol, P., Holmes, M. & Emr, S. D. (1996) *J. Biol. Chem.* **271,** 33607–33615.
21. Saurin, A. G., Borden, K. L. B., Boddy, M. D. & Freemont, P. S. (1996) *Trends Biochem. Sci.* **21,** 208–214.
22. Burd, C. R., Mustol, P. A., Schu, P. V. & Emr, S. D. (1996) *Mol. Cell. Biol.* **16,** 2369–2377.
23. Horazdovsky, B. R., Busch, G. R. & Emr, S. D. (1994) *EMBO J.* **13,** 1297–1309.
24. Rieder, S. E., Banta, L. M., Köhrer, K., McCaffery, J. M. & Emr, S. D. (1996) *Mol. Biol. Cell* **7,** 985–999.
25. Yamaguchi, Y., Heiny, M. E., Suzuki, M. & Gitlin, J. D. (1996) *Proc. Natl. Acad. Sci. USA* **93,** 14030–14055.
26. Scheckman, R. & Orci, L. *Science* (1996) **271,** 1526–1533.